RSC Advances

ROYAL SOCIETY OF CHEMISTRY

www.rsc.org/advances

Graphical Abstract

A novel adsorbent is achieved by modifying reduced graphene oxide with polymeric ionic liquid and further assembled on SiO_2 nanoparticles. This nano-hybrid exhibits selective adsorption of ovalbumin with an ultra-high sorption capacity.

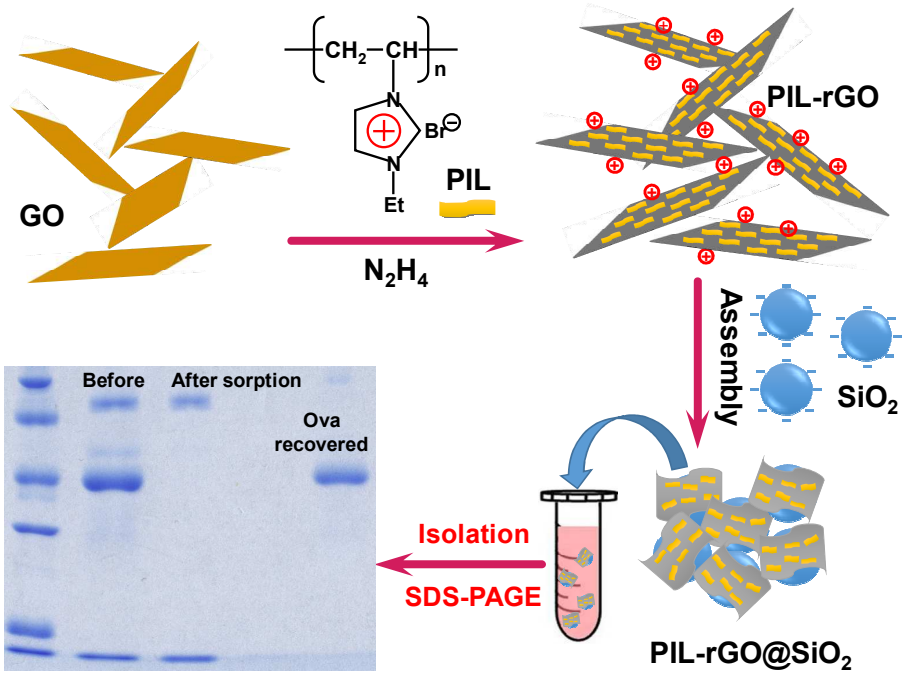

Cite this: DOI: 10.1039/c0xx00000x

www.rsc.org/xxxxxx

ARTICLE TYPE

Polymeric ionic liquid modified reduced graphene oxide as adsorbent for highly selective isolation of acidic protein

Jia-Wei Liu[a#], Meng-Meng Wang[a#], Yue Zhang[a], Lu Han[a], Xu-Wei Chen[a*], Jian-Hua Wang[a,b*]

Received (in XXX, XXX) Xth XXXXXXXXX 20XX, Accepted Xth XXXXXXXXX 20XX
DOI: 10.1039/b000000x

Polymeric ionic liquid (PIL), poly(1-vinyl-3-ethylimidazolium bromide) (P(ViEtIm$^+$Br$^-$)), modified reduced graphene oxide (rGO) nanosheets (PIL-rGO) are prepared during the reduction process by hydrazine hydrate. The as-prepared PIL-rGO is further self-assembled onto the surface of SiO_2 nanoparticles through electrostatic interactions as demonstrated by TEM & SEM images. The obtained PIL-rGO@SiO_2 nano-hybrid exhibits highly selective adsorption toward acidic protein, i.e., ovalbumin (Ova) as a model in the present case. The strong electrostatic attractions and π-π interactions between Ova and the nano-hybrid are the main driving forces for protein adsorption. An adsorption efficiency of ca. 95% is achieved for 150 mg L^{-1} Ova in a 4 mM B-R buffer at pH 5, along with an ultra-high adsorption capacity of *ca*. 917.4 mg g^{-1} as compared to those adsorbents for similar purposes. The adsorbed Ova could be effectively recovered from the surface of the nano-hybrid by using a 0.4% (w/v) SDS solution, giving rise to a recovery of ca. 70%. The practical applicability of PIL-rGO@SiO_2 nano-hybrid is demonstrated by selective isolation and removal of Ova from a complex biological sample matrix, i.e., chicken egg white.

Introduction

Graphene, a novel two-dimensional carbon-based nanomaterial, has become a "super star" in the fields of physics, chemistry and engineering during the past decade. The specific and outstanding structural, physical and chemical properties of graphene make it as a potential candidate in various applications, e.g., electronic devices, energy storage, sensors and biological investigations.[1-5] For large-scale use of graphene-based materials, one of the most common route is the oxidation and exfoliation of graphite to form graphene oxide followed by removal of the oxygen-containing groups on the surface of graphene oxide sheets by using suitable reduction reagents.[6,7] However, the strong van der Waals interactions between graphene layers after chemical conversion process result in their irreversible aggregation and poor dispersion in specific solvents. This deteriorates their applications in chemical and biological fields. A lot of efforts have been made to improve the dispersibility and solubility of graphene in aqueous medium with the assistance of organic molecules[8,9] and polymers[10-13] through covalent or non-covalent interactions during the reduction process of graphene oxide. The modification of graphene not only maintains the intrinsic properties of graphene but also increase the charge density on its surface, facilitating the stable dispersion of graphene in aqueous medium.

Polymeric ionic liquids (PILs) are a class of polyelectrolytes derived from ionic liquid monomers.[14] PILs possess both the features of ionic liquids, i.e., ionic conductivity, thermal/chemical stability and structural tunable properties, and the intrinsic properties of polymer, i.e., mechanical stability, processability, durability and spatial controllability. These provide a new family of polyelectrolytes with unique characters and broaden the range of applications.[14-16] The high charge density and rich π-electron moieties make PILs as an effective stabilizer or modifier for the functionalization of graphene nanosheets, and the PILs modified graphene nanosheets exhibit high solubility and stability in various solvent media.[17-19] Besides, the PILs-graphene composite offers enhanced compatibility with ionic liquid and a stable electrochemical response, giving rise to a favorable potential in high-performance supercapacitors.[20] Moreover, the tunable cationic and anionic moieties in the PILs structures improve the reversible phase transfer of graphene sheets between water and organic solvents, which might facilitate their applications in organic electronics.[21] In general, the combination of PILs with graphene nanosheets exhibits both the advantages of PILs and graphene nanosheets. In the meantime, the stability of graphene in various solvents has been improved. Nevertheless, it should be noted that so far nanocomposite of PIL and graphene has not been applied to the adsorption of proteins in biological systems.

Acidic proteins have low isoelectric points and are generally negatively charged under physiological condition (pH 7.4). For proteomic research, it is desired to obtain high purity of protein from biological samples, and thus appropriate isolation processes are necessary. Typically, two acidic proteins, e.g., bovine serum albumin (BSA) and Ovalbumin (Ova), are usually employed as models for the investigation of acidic protein isolation. Various materials have been developed as sorbents for selective isolation of acidic proteins. Poly(diallyldimethylammonium chloride) (PDDA) functionalized multi-walled carbon nanotubes (MCNTs) have been used for on-line selective isolation of BSA from human whole blood. [22] On the other hand, Ova has been selectively isolated from chicken egg white by use of polymeric ionic liquid cross-linked silica nanoparticles as sorbent. [23]

In the present work, reduced graphene oxide (rGO) nanosheets are functionalized with a polymeric ionic liquid (PIL), poly(1-vinyl-3-ethylimidazolium bromide) (P(ViEtIm$^+$Br$^-$)), to produce a PIL-rGO nanocomposite. The PIL-rGO nanocomposite is then assembled onto the surface of nano-sized silica particles to achieve a PIL-rGO@SiO_2 nano-hybrid. The immobilization of graphene-based nanomaterials onto silica particles or solid supports is a useful strategy to overcome the poor recovery of graphene/graphene oxide nanosheets from aqueous medium and to make it ease of operation in the commonly adopted adsorption-desorption/recovery process in separation science.[24,25] The obtained PIL-rGO@SiO_2 nano-hybrid is for the first time used as a novel adsorbent for the highly selective isolation of acidic protein (ovalbumin) from complex sample matrix, i.e., chicken egg white in the present case. The various parameters governing the adsorption of protein species are carefully investigated and the practical applications of PIL-rGO@SiO_2 nano-hybrid for selective isolation of acidic protein is demonstrated by SDS-PAGE assay.

Experimental

Chemicals and Materials

High purity graphite powder (spectral grade), *N*-vinylimidazole, bromoethane, tetraethoxysilane (TEOS) hydrazine hydrate ($N_2H_4 \cdot H_2O$, 85%) and sodium dodecylsulfate (SDS) are purchased from Sinopharm Chemical Reagent Co. Ltd. (Shanghai, China). 2,2'-azobisisobutyronitrile (AIBN) is obtained from Shanghai No.4 Reagent & H.V. Chemical Co., Ltd. (Shanghai, China). Acetonitrile, anhydrous ethanol, chloroform, ethyl acetate and ammonium hydroxide ($NH_3 \cdot H_2O$, 25%) are supplied by Bodi Chemical Holding Co. Ltd. (Tianjin, China). Other reagents including potassium permanganate, sulfuric acid, sodium nitrate, hydrochloric acid and hydrogen peroxide (H_2O_2, 30%) are received from Damao Chemical Reagent Factory (Tianjin, China). All the chemicals used are at least of analytical reagent grade and are used as received without further purification. 18 MΩ cm deionized water is used throughout.

Ovalbumin (Ova, A5503, >98%) and lysozyme (Lys, L2879, Grade VI) are purchased from Sigma-Aldrich (St. Louis, USA) and used without further treatment. The protein molecular weight marker (low, D530S, Takara Biotechnology Company, Dalian, China) is a mixture of six purified proteins (Mr in kDa: phosphorylase B, 97.2; serum albumin, 66.4; ovalbumin, 44.3; carbonic anhydrase, 29; trypsin inhibitor, 20.1; lysozyme, 14.3).

The protein stock solutions of 1.0 mg mL^{-1} are prepared by dissolving certain amount of proteins in buffers with various pH values and the working solutions are obtained by stepwise dilution of the stock solutions with corresponding buffers. In this case, Britton-Robinson (B-R) buffers are employed to investigate the adsorption behaviors of Ova and Lys on the PIL-rGO@SiO_2 nano-hybrid. Typically, 4 mM acetic acid, phosphoric acid and boric acid are mixed together and the pH values are adjusted by using a 0.2 mol L^{-1} NaOH solution. A sodium dodecylsulfate (SDS) aqueous solution of 0.4% (w/v) is employed as eluent/stripping solution for the recovery of adsorbed protein.

Preparation of PIL-rGO@SiO_2 nnao-hybrid

Preparation of ViEtIm$^+$Br$^-$ monomer: Ionic liquid monomer ViEtIm$^+$Br$^-$ is prepared according to the literature.[26] Briefly, 40 mL of *N*-Vinylimidazole (41.52 g, 0.44 mol) is transferred into a 250-mL round-bottom flask, and 50 mL of bromoethane (73.06 g, 0.67 mol) is drop-wisely added under vigorous stirring. Then the mixture is refluxing at 70□ for 12 h. After phase separation, the supernatant is removed and 20 mL of acetonitrile is added for further refluxing at 80□ for 1 h. Afterwards the viscous liquid is transferred into a 500-mL beaker and *ca.* 1.0 mL of ethyl acetate are dropwisely added for the recrystallization at -20□. Finally, the ViEtIm$^+$Br$^-$ monomer is obtained after filtering, washing and drying under vacuum.

Preparation of P(ViEtIm$^+$Br$^-$) polymer: Typically, 2.0 g of ViEtIm$^+$Br$^-$ monomer is dissolved in 20 mL of chloroform and 0.04 g of AIBN is added as an initiating agent. The polymerization is taken place at 70□ for 3 h under nitrogen protection. Afterwards, the product is transferred into a 250-mL beaker and dried under vacuum at room temperature.

Preparation of PIL-rGO nanocomposite: Grpahene oxide (GO) is prepared by following the modified Hummers' method as described in our previous work.[27] A yellow-brown graphene oxide suspension (1.0 mg mL^{-1}) is obtained by mild sonication of certain amount of graphite oxide in water. The PIL-rGO nanocomposite is prepared as follows: firstly, 0.3 g of P(ViEtIm$^+$Br$^-$) is dissolved in 25 mL of water, and then 15 mL of graphene oxide aqueous solution (15 mg) is added. After the addition of 45 μL of hydrazine hydrate, the mixture is refluxing at 95□ for 24 h. At last, the black product is centrifuged, washed with water for three times, and freeze-dried under vacuum for 12 h.

Preparation of nano-sized silica particles: The synthesis of SiO_2 nanoparticles follows the classic Stober method.[28] Shortly, 100 mL of anhydrous ethanol, 11 mL of water and 6 mL of ammonium hydroxide are mixed in a 250-mL round-bottom flask under magnetic stirring to form a homogenous solution. Then 6 mL of TEOS is added into the above solution, and the hydrolyzation is occurred at 30□ for 24 h. The product is collected by centrifugation at 5000 rpm for 5 min, washed with water for three times, and dried under vacuum.

Self-assembly of PIL-rGO onto SiO_2 nanoparticles: PIL-rGO could be self-assembled onto the surface of SiO_2 nanoparticles through electrostatic attractions. Firstly, PIL-rGO and SiO_2 nanoparticles are dispersed in water by mild sonication to obtain homogenous solutions/suspensions of 1.0 mg mL^{-1} for PIL-rGO and 10 mg mL^{-1} for SiO_2 nanoparticles. The solutions are then mixed together with a volume ratio of 7:1 (PIL-rGO/SiO_2) and the mixture is continuously stirred at room temperature for 1 h to facilitate assembly of PIL-rGO onto the surface of SiO_2 nanoparticles. The final product, PIL-rGO@SiO_2 nano-hybrid, is collected by centrifugation, washed with water, and freeze-dried under vacuum.

Characterizations

Fourier transform infrared (FT-IR) spectra of GO, P(ViEtIm$^+$Br$^-$) and PIL-rGO are recorded by using a Nicolet-6700 FT-IR spectrophotometer (Thermo Fisher Scientific, USA) from 500 to 4000 cm^{-1}. UV-Vis spectra of GO, P(ViEtIm$^+$Br$^-$) and PIL-rGO are performed on a U-3900 UV-Vis spectrophotometer (Hitachi

High Technologies, Japan) from 190-600 nm with 1-cm quartz cuvette. TEM images are recorded on an H-7650 microscope with an accelerating voltage of 80 kV (Hitachi High Technologies, Japan). The morphologies of SiO_2 nanoparticles and PIL-rGO@SiO_2 nano-hybrid are measured by S-3400N scanning electronic microscopy (SEM, Hitachi High Technologies, Japan). The thermogravimetric analysis (TGA) is carried out by a TGA/DSC 1 STARe System (Mettler-Toledo, Switzerland) from 25 to 500□ with a heating rate of 10□ min^{-1} in nitrogen atmosphere. Raman spectra of graphite powder, GO and PIL-rGO are performed on a LabRAM XploRA Raman microscope (HORIBA Jobin Yvon, France) with excitation laser wavelength at 638 nm. The zeta potential analysis for PIL-rGO with various mass ratios of PIL and GO are conducted on Zetasizer Nano ZS90 (Malvern, UK).

Adsorption of proteins with the PIL-rGO@SiO_2 nano-hybrid

In this work, Ova (pI 4.7) and Lys (pI 10.5-11) are employed as the model proteins to investigate their adsorption behaviors on the surface of PIL-rGO@SiO_2 nano-hybrid within pH 3-12. Generally, 3.0 mg of PIL-rGO@SiO_2 nano-hybrid is added into a protein sample solution (150 mg L^{-1}, 1.0 mL) and the mixture is shaken vigorously for 30 min to facilitate the protein adsorption process. After adsorption, the mixture is centrifuged at 8000 rpm for 5 min and the supernatant is collected to quantify the residual proteins in the aqueous medium by using a U-3900 UV-Vis spectrophotometer (Hitachi High Technologies, Japan).

The adsorbed protein species are efficiently recovered from the surface of PIL-rGO@SiO_2 nano-hybrid by using a 0.4% (w/v) of SDS aqueous solution. Briefly, 1.0 mL of SDS solution is mixed with PIL-rGO@SiO_2 nano-hybrid and then continuously oscillated for 30 min to facilitate the stripping/desorption of the proteins retained on the surface of the nano-hybrid. The supernatant with recovered proteins is collected by centrifugation at 8000 rpm for 5 min and stored in refrigerator for ensuing investigations.

Isolation of ovalbumin from chicken egg white

Chicken egg white is obtained from fresh eggs. It is 200-fold diluted with 4 mM B-R buffer at pH 5 followed by gently stirring to form a homogeneous solution. Afterwards, the supernatant is collected by centrifugation at 8000 rpm for 20 min for performing protein adsorption/isolation as described in the previous section. Considering that the concentration of lysozyme in 200-fold diluted solution is very low, its band might not appear in the SDS-PAGE assay, a standard lysozyme solution of 100 mg L^{-1} is spiked into the original solution. After the adsorption process, the surface of the nano-hybrid is washed by 1.0 mL of 4 mM B-R buffer at pH 5 to eliminate the loosely retained interfering components. The retained Ova is then recovered by stripping with 1 mL of 0.4% (m/v) SDS solution. All the supernatants for each step are collected into 1.5-mL plastic tubes for SDS-PAGE assay, which is performed by using 12% polyacrylamide resolving gel and 5% polyacrylamide stacking gel with standard discontinuous buffer systems.

Results and discussion

Preparation and Characterization of PIL-rGO@SiO_2 nano-hybrid

The preparation procedures for P(ViEtIm$^+$Br$^-$), PIL-rGO nanosheets and PIL-rGO@SiO_2 nano-hybrid are illustrated in Scheme 1. Firstly, ionic liquid monomer is obtained through a universal process for imidazoium ionic liquid preparation.[29] Then the polymerization is taken place among the vinyl groups of the cationic moieties of ionic liquid with the assistance of AIBN (Scheme 1a). The P(ViEtIm$^+$Br$^-$) dissolves in water due to the abundant hydrophilic IL moieties in the P(ViEtIm$^+$Br$^-$) framework, which is benefit for the surface functionalization of graphene oxide in aqueous medium. Secondly, graphene oxide is reduced by hydrazine hydrate to form reduced graphene oxide (rGO), meanwhile the P(ViEtIm$^+$Br$^-$) is assembled onto the surface of rGO nanosheets through strong π-π interactions between the imidazolium cations of P(ViEtIm$^+$Br$^-$) and rGO nanosheets.[19] The P(ViEtIm$^+$Br$^-$) significantly improves the solubility and stability of rGO nanosheets in water attributed to the high charge density on the surface of PIL-rGO. On the other hand, however, these features make it difficult to manipulate the highly soluble PIL-rGO during the protein adsorption/desorption process. In the present case, this problem is solved by assembling the PIL-rGO onto silica nanoparticles. In fact, the abundant imidazolium cations in the PIL framework provide positive charges (zeta potential at +62 mV) while the SiO_2 nanoparticles are negatively charged (zeta potential at -50 mV). The opposite surface charge properties obviously facilitate the self-assembly of PIL-rGO onto the surface of SiO_2 nanoparticles through electrostatic interactions.

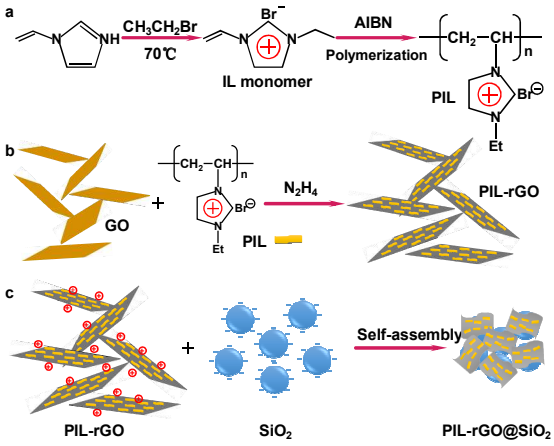

Scheme 1 The schemes for the preparation of (a) P(ViEtIm$^+$Br$^-$), (b) PIL-rGO, and (c) PIL-rGO@SiO_2 nano-hybrid.

In order to achieve effective coverage of P(ViEtIm$^+$Br$^-$) onto the surface of rGO nanosheets, the PIL-rGO are prepared by varying the mass ratio of P(ViEtIm$^+$Br$^-$) and graphene oxide at 1/1, 5/1, 10/1, 20/1, 40/1 and 50/1, and the zeta potentials of the products are then evaluated. It is illustrated in Fig. S1 (Supporting Information) that the increase of mass ratio from 1/1 up to 20/1 results in a significant improvement on the zeta potential of PIL-rGO from +37 to +62 mV, this is a clear indication for the adhesion of more P(ViEtIm$^+$Br$^-$) moieties onto the surface of rGO nanosheets through π-π interactions. When further increasing the mass ratio to >20/1, the improvement on surface charge is

marginal, that is the zeta potential of PIL-rGO is maintained at the level close to that for pure P(ViEtIm$^+$Br$^-$) at ca. +66 mV. This observation demonstrates that the surface of rGO nanosheets have been completely covered by the P(ViEtIm$^+$Br$^-$) moieties. For the ensuing investigations, a mass ratio of P(ViEtIm$^+$Br$^-$)/GO=20/1 is adopted.

Fig. 1A illustrates the FT-IR spectra of GO, P(ViEtIm$^+$Br$^-$) and PIL-rGO. In the spectrum of GO (a), three typical absorption bands of C=O (carboxyl) at 1725 cm^{-1}, C-O-C (epoxide) at 1230 cm^{-1} and C-O (hydroxyl) at 1070 cm^{-1} are observed, which are introduced on the surface and/or at the edge of GO platelets during the oxidation process of graphite. After the reduction process, the absorption bands corresponding to these oxygen-functional groups disappear and/or weaken in the spectrum of PIL-rGO (c), demonstrating partial reduction of graphene oxide by hydrazine hydrate. Meanwhile, the characteristic vibration bands attributed to imidazolium cations at 1547, 1450 and 1160 cm^{-1} are observed in the spectrum of PIL-rGO. These absorption bands are almost the same as those for P(ViEtIm$^+$Br$^-$) (b). Moreover, the new stretching vibration bands of C-H groups within 2800-3200 cm^{-1} are derived from the vinyl and ethyl groups of P(ViEtIm$^+$Br$^-$) frameworks (c). The observations indicate that the assembly of P(ViEtIm$^+$Br$^-$) onto the surface of rGO nanosheets is achieved.

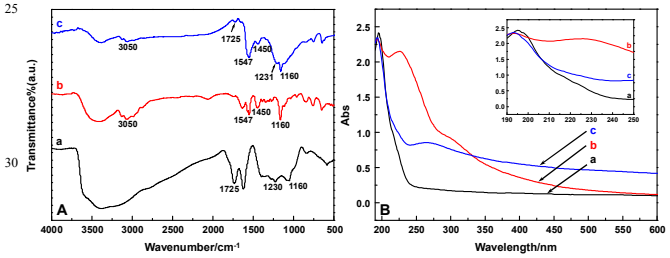

Fig. 1 (A) FT-IR spectra of (a) GO, (b) P(ViEtIm$^+$Br$^-$) and (c) PIL-rGO; (B) UV-Vis spectra of (a) P(ViEtIm$^+$Br$^-$), (b) GO and (c) PIL-rGO.

UV-Vis spectra of P(ViEtIm$^+$Br$^-$), GO and PIL-rGO in aqueous medium are shown in Fig. 1B. GO exhibits a distinct absorption at 228 nm, which is attributed to the π-π* transition of C=C band (b).[30] This absorption peak is red-shifted to 270 nm in the spectrum of PIL-rGO, probably due to the deoxygenation and partial restoration of the electronic conjugation during the reduction process (c).[30] For the case of P(ViEtIm$^+$Br$^-$), it seems that there is no obvious absorption in a wide range of UV-Vis region and the maximum absorption is located in the far ultraviolet region, i.e., 195 nm (a). When modifying this polymer onto the surface of rGO nanosheets, a tiny blue-shift from 195 to 193 nm is observed (curve a and c in the insert of Fig. 2B) due to the π-π interactions between P(ViEtIm$^+$Br$^-$) and rGO nanosheets. The UV-Vis spectra further demonstrate the successful preparation of PIL-rGO.

Raman spectroscopy is employed to investigate the changes in graphitic structures during oxidation and reduction processes. As shown in Fig. 2, bulk graphite usually exhibits a typical G band (~1583 cm^{-1}) and 2D band (~2700 cm^{-1}), which are ascribed to the doubly degenerate zone center E_{2g} mode of all pairs of sp^2 carbon atoms and the second order of zone-boundary phonons, respectively (Fig. 2a).[31,32] Moreover, a small speak at round 1330 cm^{-1}, namely D band, is observed and indicated the existence of sp^3 hybridized carbon atoms and other defects in the graphite sample.[33] The intensity ratio of D and G band (I_D/I_G) is used to measure the disorder in the samples and a I_D/I_G value of 0.05 for bulk graphite is obtained. The oxidation of graphite results in a significant increase of the intensity of D band and disappearance of 2D band in the spectrum of GO (Fig. 2b). Besides, the I_D/I_G value for GO is also sharply increased to 0.98 in comparison with that of bulk graphite. These observations suggest that the sp^2 hybridized structure is partly damaged during the oxidation process, and more sp^3 hybridized carbon atoms are formed on GO platelets. After the reduction by hydrazine hydrate and PIL modification, the I_D/I_G value for PIL-rGO (Fig. 2c) is further increased to 1.12, indicating that an increase in number while a decrease in the average size of sp^2 domains upon reduction.[6] Furthermore, the similar Raman peaks of PIL-rGO nanosheets as those of GO demonstrate that the graphitic structure of PIL-rGO nanosheets could be maintained in the presence of PIL moieties.

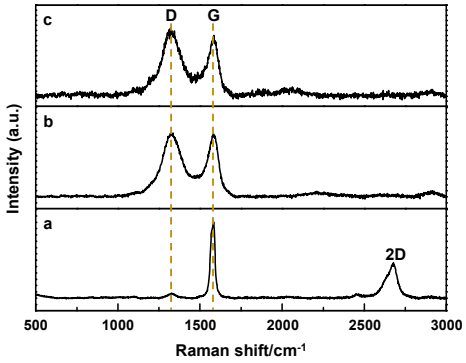

Fig. 2 Raman spectra of (a) graphite powder, (b) GO and (c) PIL-rGO.

The thermal properties of rGO, P(ViEtIm$^+$Br$^-$) and PIL-rGO are investigated by thermogravimetric analysis (TGA) and the results are shown in Fig. 3. It is seen that the thermal decomposition of rGO is taken place within 100-250℃ and the main mass loss (*c.a.* 15%) is derived from the unstable oxygen-containing groups on the rGO nanosheets (Fig. 3a). The TG curve of rGO indicates a partial removal of oxygen-containing groups from the surface of GO under the present reduction procedure. For pure P(ViEtIm$^+$Br$^-$), it is stable at lower temperature (<270℃), and only 10% of mass loss is obtained under 100℃ because of the evaporation of adsorbed water molecules. The pyrolysis of P(ViEtIm$^+$Br$^-$) is mainly occurred at around 300℃ and a mass loss of *c.a.* 74% is achieved, which is in agreement with the previous work (Fig. 3b).[34] PIL-rGO shows thermal stability below 250℃ (Fig.3c), and the mass loss of *c.a.* 60% at around 300℃ is ascribed to the decomposition of P(ViEtIm$^+$Br$^-$) moieties. TG analysis results demonstrate successful modification of rGO with P(ViEtIm$^+$Br$^-$) and the thermal stability of rGO could be improved.

The assembly of PIL-rGO nanosheets onto the surface of SiO_2 nanoparticles is demonstrated by TEM and SEM images. As illustrated in Fig. 4a and c, pure silica nanoparticles are ideally spherical with uniform size and smooth surface. The average diameter of silica nanoparticles is 265 nm. After the assembly process, the shape and size of silica nanoparticles keep the same while their surfaces are encapsulated by crumpled and ultrathin PIL-rGO nanosheets (see arrows in Fig. 4b). Moreover, the edges

of PIL-rGO nanosheets are spread out of the spheres to a large extent without agglomeration, thus keeping the high surface area of PIL-rGO and providing abundant adsorption sites for protein species.[35] In addition, the SEM image of PIL-rGO@SiO_2 nano-hybrid further demonstrates the effective assembly of PIL-rGO nanosheets onto silica nanoparticles through electrostatic interactions (see arrows in Fig. 4d).

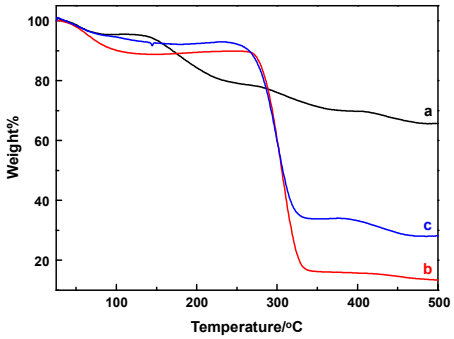

Fig. 3 TGA curves of (a) rGO, (b) P(ViEtIm$^+$Br$^-$) and (c) PIL-rGO.

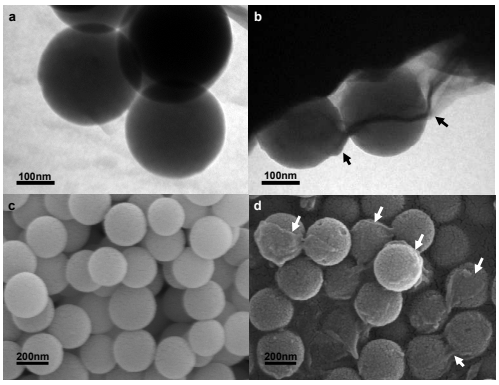

Fig. 4 TEM and SEM images of pure SiO_2 nanoparticles (a,c) and PIL-rGO@SiO_2 nano-hybrid (b,d).

Protein adsorption with the PIL-rGO@SiO_2 nano-hybrid as adsorbent

The PIL-rGO@SiO_2 nano-hybrid is employed as adsorbent for protein adsorption and separation. In the present case, Ova and Lys are employed as two model proteins to evaluate the adsorption behaviors of the PIL-rGO@SiO_2 nano-hybrid. Fig. 5A shows the adsorption performances of the two proteins on the PIL-rGO@SiO_2 nano-hybrid within a wide pH range. It is obvious that an increase of adsorption efficiency for Ova is achieved with the increase of pH value from 3 to 5, and then a favorable adsorption efficiency of >90% is maintained within pH 5-10. Thereafter, a decline of the adsorption efficiency is observed when further increasing to pH 12. The surface charge properties of the PIL-rGO@SiO_2 nano-hybrid at various pH values are measured and the results are shown in Table S1. It is clearly seen that the surface of PIL-rGO@SiO_2 nano-hybrid is positively charged within the whole pH range tested, thus electrostatic interactions between the nano-hybrid and Ova might be the main driving force to facilitate the protein adsorption. It is known that the isoelectric point (pI) value of Ova is 4.7, suggesting that the surface of Ova is negatively charged in the range of pH 5-12. Therefore, the strong electrostatic attractions between Ova and the nano-hybrid facilitate Ova adsorption. At a high pH value, e.g., pH 11-12, the abundant anions in the buffer might neutralize the surface of the nano-hybrid, which might weaken the electrostatic attractions and result in the decline of adsorption efficiency. In contrast, at a pH value lower than the pI of Ova, e.g., pH 3-4, Ova turns to be positively charged and the electrostatic repulsion deteriorates its adsorption on the PIL-rGO@SiO_2 nano-hybrid.

For the case of Lys, it is obvious that the adsorption efficiency is much lower in comparison with that of Ova, and it exhibits a slight improvement with the increase of pH value. This result demonstrates that electrostatic interactions also donate the adsorption of Lys onto the surface of PIL-rGO@SiO_2 nano-hybrid. Considering that the isoelectric point of Lys is pI 10.5~11, both Lys and the nano-hybrid are positively charged in a wide range of pH 3-11, thus electrostatic repulsions deteriorate the adsorption of Lys, giving rise to a lower adsorption efficiency. The slight increase of adsorption efficiency with the increase of pH value is ascribed to the decrease of the positive charges on the surface of both Lys and PIL-rGO nano-hybrid. As pH>pI, Lys turns to be negatively charged and more Lys molecules are adsorbed onto the PIL-rGO nano-hybrid through electrostatic interactions. Furthermore, it is noticed that at pH 5 there is a significant difference on the adsorption of Ova and Lys by the PIL-rGO@SiO_2 nano-hybrid, this provides a promising potential for selective separation of these proteins or removal of abundant protein species, e.g., Ova in this case, by using the PIL-rGO@SiO_2 nano-hybrid as adsorbent.

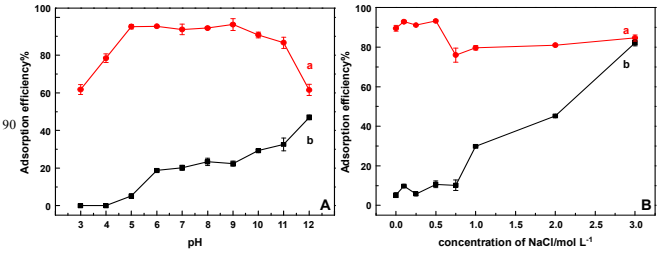

Fig. 5 (A) pH dependent adsorption efficiencies of protein species onto the PIL-rGO@SiO_2 nano-hybrid: (a) Ova and (b) Lys. (B) Effect of ionic strength on the adsorption efficiencies of proteins: (a) Ova and (b) Lys. The concentration and volume of protein sample: 150 mg L^{-1} and 1.0 mL; Amount of PIL-rGO@SiO_2 nano-hybrid: 3 mg; Adsorption time: 30 min.

For further investigation of mechanism for protein adsorption on the nano-hybrid, the effect of ionic strength on the adsorption efficiency is studied in the presence of NaCl with concentrations in a range of 0.0-3.0 mol L^{-1} at pH 5. As shown in Fig. 5B, it seems that the adsorption of Ova on the nano-hybrid is not very sensitive with the variation of ionic strength. This result indicates that there is an alternative binding force between protein and the nano-hybrid. As is known that both imidazolium in PIL and rGO contain π-rich moieties, which implies that the strong π-π interactions between PIL/rGO and the residual amino acids in Ova molecules provide another contribution for Ova adsorption. Moreover, a decline of adsorption efficiency at an ionic strength of 0.75 mol L^{-1} NaCl is observed because the presence of NaCl might cause negative effect on the electrostatic attractions between Ova and the nano-hybrid. In contract, the adsorption of Lys on the nano-hybrid is increased obviously at a higher ionic

strength. As discussed previously, the electrostatic repulsions dominate the adsorption process of Lys at pH 5, and the increase of ionic strength might weaken the repulsions between Lys and the nano-hybrid and thus facilitate its adsorption.[36] Meanwhile, there are also π-π interactions between Lys and the PIL-rGO@SiO_2 nano-hybrid, which could be strengthened by increasing the ionic strength. The above observations demonstrate that electrostatic forces and π-π interactions are the main binding forces for protein adsorption on the nano-hybrid.

The adsorption of Ova and Lys is further investigated at pH 5 by use of pure SiO_2 nanoparticles, rGO nanosheets and PIL-rGO@SiO_2 nano-hybrid. As shown in Table S2, both Ova and Lys could be adsorbed on pure SiO_2 and rGO nanosheets with high efficiencies while PIL-rGO@SiO_2 nano-hybrid exhibits high selectivity toward Ova. This observation clearly demonstrates that the modification of rGO by PIL significantly improves the selectivity of graphene-based composite material toward specific proteins and the assembly of PIL-rGO onto SiO_2 nanoparticles effectively eliminates non-specific adsorption of proteins on SiO_2 surface.

Adsorption of Ova on PIL-rGO@SiO_2 nano-hybrid

As discussed previously that selective adsorption is achieved on PIL-rGO@SiO_2 nano-hybrid in a B-R buffer at pH 5. A maximum adsorption efficiency of ca. 95% for Ova is achieved, while in the meantime the adsorption of Lys is negligible. The adsorption capacity is evaluated by performing the adsorption at room temperature within a Ova concentration range of 50-5000 mg L^{-1}, and the adsorption isotherm of Ova on the nano-hybrid is illustrated in Fig. S2. It is seen that a rapid increase of the amount of Ova adsorbed on PIL-rGO@SiO_2 nano-hybrid is observed when increasing its concentration up to 3500 mg L^{-1}. Thereafter, a plateau is achieved and maintained at an even higher concentration of Ova. The experimental data fit the *Langmuir* theoretical adsorption model, as characterized by the following equation:[23]

$$\frac{C_e}{Q_e} = \frac{C_e}{Q_{max}} + \frac{1}{b \cdot Q_{max}}$$

C_e and Q_e are equilibrium concentration (mg L^{-1}) and adsorption capacity at equilibrium concentration (mg g^{-1}), Q_{max} is the therotetical maximum adsorption capacity (mg g^{-1}), and b is adsorption equilibrium constant (mL mg^{-1}).

In the present case, a linear equation is derived as in the following. A maximum adsorption capacity of 917.4 mg g^{-1} for Ova is derived from the reciprocal of intercept value.

$1/Q_e=0.1808\times1/C_e+0.00109$ ($R^2>0.99$).

Table 1 lists the adsorption capacities of Ova on various adsorbent materials, and it is obvious that PIL-rGO@SiO_2 nano-hybrid provides a much higher adsorption capacity with respect to others reported so far in the literature. This might be partly attributed to the specific and huge surface area of graphene-based materials.[40] The ultra-high adsorption capacity of Ova by the PIL-rGO@SiO_2 nano-hybrid makes it as an effective adsorbent for the removal of abundant protein species from complex sample matrixes.

Table 1. Comparisons of adsorption capacities for Ova on various adsorbent materials.

Adsorbent	Adsorption capacity mg g^{-1}	Ref.
Macroporous molecularly imprinted cryogel	23.0	37
Statobind phenyl™ membrane	42.7[a]	38
Clay mineral	272.4	39
PIL@SiO_2	333.3	23
PIL-rGO@SiO_2 nano-hybrid	917.4	This work

[a]mg mL^{-1}

Generally, for further life science investigations, the adsorbed protein on the surface of adsorbent should be recovered or collected. In the present case, Ova is effectively adsorbed by the PIL-rGO@SiO_2 nano-hybrid within a wide pH range and ionic strength, which implies that playing with pH value and/or ionic strength in the stripping agent will not work for the collection/recovery of Ova. Considering that SDS is a universal stripping reagent for protein recovery from ionic liquid-based adsorbent materials,[23,41] a dilute SDS solution is employed for Ova recovery from the surface of the PIL-rGO@SiO_2 nano-hybrid. Fig. 6 illustrates the effect of SDS concentration on the recovery of Ova. It is clearly observed that the recovery of Ova is improved obviously with the increase of SDS concentration, and a maximum recovery of ca. 80% is obtained at a SDS concentration of 0.8% (w/v). A further increase of SDS concentration up to 1.0% results in a slight decline of the recovery. Considering that SDS is a strong anionic surfactant, which tends to cause conformational change of proteins at high concentration.[23] Therefore, a 0.4% (w/v) of SDS solution is selected for the recovery of Ova in the present case, giving rise to a recovery of ca. 70%.

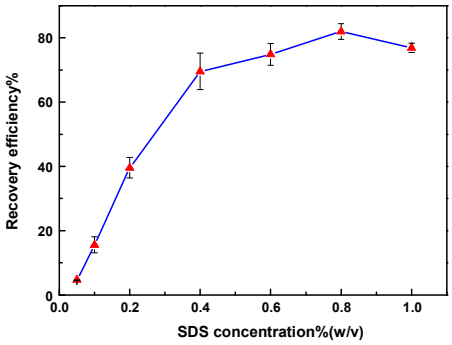

Fig. 6 The dependence of Ova recovery from the PIL-rGO@SiO_2 nano-hybrid on SDS concentration. Adsorption: 1.0 mL of 150 mg L^{-1} Ova solution in 4 mM B-R buffer at pH 5 with 3 mg of PIL-rGO@SiO_2 nano-hybrid; elution: 1.0 mL of SDS solution with various concentrations; Adsorption and elution time: 30 min for each.

Isolation and removal of Ova from chicken egg white

The practical applicability of the PIL-rGO@SiO_2 nano-hybrid as adsorbent for protein isolation is investigated by performing adsorption of Ova from complex matrix sample, i.e., chicken egg white. The results are demonstrated by SDS-PAGE assay, as illustrated in Fig. 7. It is clear that a few protein bands are observed in the chicken egg white sample (Lane 2), which might be derived from conalbumin, Ova and Lys. After the adsorption process, the Ova band disappears while others remain virtually unchanged in the supernatant (Lane 3). This obviously indicates that the PIL-rGO@SiO_2 nano-hybrid exhibits high selectivity

toward adsorption of Ova. After performing a washing step (Lane 4), a single band is observed in the eluent (Lane 5) located at the same position as that for standard Ova at ca. 44.3 kDa (Lane 6). The SDS-PAGE results well demonstrate that Ova is selectively isolated from chicken egg white in the presence of other protein species. This observation provides a useful approach for the selective removal of abundant proteins from complex sample matrixes.

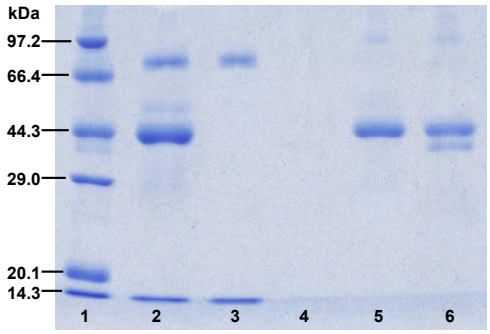

Fig. 7 SDS-PAGE assay results. Lane 1: molecular weight standards (Marker in kDa); Lane 2: 200-fold diluted chicken egg white spiked with 100 mg L^{-1} Lys; Lane 3: the supernatant after adsorption by PIL-rGO@SiO_2 nano-hybrid; Lane 4: washing solution by 4 mM B-R buffer at pH 5; Lane 5: Ova recovered from the PIL-rGO@SiO_2 nano-hybrid; Lane 6: Ova standard solution of 360 mg L^{-1}.

Conclusion

In this work, polymeric ionic liquid modified reduced graphene oxide (PIL-rGO) are synthesized and it is further assembled onto the surface of SiO_2 nanoparticles via electrostatic interactions, and the obtained PIL-rGO@SiO_2 nano-hybrid provides a novel adsorbent for highly selective adsorption of Ova. The presence of PIL significantly improves the solubility and stability of rGO and offers favorable selectivity on the adsorption of specific protein by the graphene-based material. In addition, the assembly of PIL-rGO nanosheets onto SiO_2 nanoparticles effectively eliminates non-specific adsorption of proteins on SiO_2 surface. Meanwhile, the specific and huge surface area of graphene provides plenty of binding sites for proteins, facilitating an ultra-high adsorption capacity toward Ova. The hyphenation of PILs and graphene nanosheets opens a new avenue for the development of biomaterials for the purpose of selective isolation of biomacromolecules and/or effective removal of high abundant protein species from complex sample matrixes.

Acknowledgments

This work is financially supported by the Natural Science Foundation of China (21275027, 21235001 and 21375013), the Program of New Century Excellent Talents in University (NCET-11-0071) and Fundamental Research Funds for the Central Universities (N110805001, N120605002, N120405004, N130105002 and N120605001).

Notes and references

[#] *These authors contribute equally to this work.*
[a] *Research Center for Analytical Sciences, Colleges of Sciences, Box 332, Northeastern University, Shenyang, 110819, China. Fax: 86 24 83676698; Tel: 86 24 83688944; E-mail: chenxw@mail.neu.edu.cn; jianhuajrz@mail.neu.edu.cn.*
[b] *Collaborative Innovation Center of Chemical Science and Engineering, Tianjin, 300071, China*

1. Y. W. Zhu, S. Murali, W. W. Cai, X. S. Li, J. W. Suk, J. R. Potts, R. S. Ruoff, *Adv. Mater.*, 2010, **22**, 3906.
2. C. Biswas, Y. H. Lee, *Adv. Funct. Mater.*, 2011, **21**, 3806.
3. L. M. Dai, *Acc. Chem. Res.*, 2013, **46**, 31.
4. H. J. Jiang, *Small*, 2010, **7**, 2413.
5. J. L. Li, B. Tang, B. Yuan, L. Sun, X. G. Wang, *Biomaterials*, 2013, **34**, 9519.
6. S. Stankovich, D. A. Dikin, R. D. Piner, K. A. Kohlhaas, A. Kleinhammes, Y. Y. Jia, Y. Wu, S. T. Nguyen, R. S. Ruoff, *Carbon*, 2007, **45**, 1558.
7. H. J. Shin, K. K. Kim, A. Benayad, S. M. Yoon, H. K. Park, I. S. Jung, M. H. Jin, H. K. Jeong, J. M. Kim, J. Y. Choi, Y. H. Lee, *Adv. Funct. Mater.*, 2009, **19**, 1987.
8. Y. C. Si, E. T. Samulski, *Nano Lett.*, 2008, **8**, 1679.
9. H. F. Yang, C. S. Shan, F. H. Li, D. X. Han, Q. X. Zhang, L. Niu, *Chem. Commun.*, 2009, **45**, 3380.
10. S. Stankovich, R. D. Piner, X. Q. Chen, N. Q. Wu, S. T. Nguyen, R. S. Ruoff, *J. Mater. Chem.*, 2006, **16**, 155.
11. X. F. Zhou, Z. P. Liu, *Chem. Commun.*, 2010, **46**, 2611.
12. X. Y. Qi, K. Y. Pu, X. Z. Zhou, H. Li, B. Liu, F. Boey, W. Huang, H. Zhang, *Small*, 2010, **6**, 663.
13. A. J. Patil, J. L. Vickery, T. B. Scott, S. Mann, *Adv. Mater.*, 2009, **21**, 3159.
14. S. Amajjahe, H. Ritter, *Macromol. Rapid Commun.*, 2009, **30**, 94.
15. D. Mecerreyes, *Prog. Polym. Sci.*, 2011, **36**, 1629.
16. J. Y. Yuan, M. Antonietti, *Polymer*, 2011, **52**, 1469.
17. Q. Zhang, S. Y. Wu, L. Zhang, J. Lu, F. Verproot, Y. Liu, Z. Q. Xing, J. H. Li, X. M. Song, *Biosens. Bioelectron.*, 2011, **26**, 2632.
18. T. T. Tung, T. Y. Kim, J. P. Shim, W. S. Yang, H. Kim, K. S. Suh, *Org. Electron.*, 2011, **12**, 2215.
19. X. S. Zhou, T. B. Wu, K. L. Ding, B. J. Hu, M. Q. Hou, B. X. Han, *Chem. Commun.*, 2010, **46**, 386.
20. T. Y. Kim, H. W. Lee, M. Stoller, D. R. Dreyer, C. W. Bielawski, R. S. Ruoff, K. S. Suh, *ACS Nano*, 2011, **5**, 436.
21. T. Y. Kim, H. W. Lee, J. E. Kim, K. S. Suh, *ACS Nano*, 2010, **4**, 1612.
22. Z. Du, Y. L. Yu, J. H. Wang, *Macromol. Biosci.*, 2009, **9**, 55.
23. L. Han, Y. Shu, X. F. Wang, X. W. Chen, J. H. Wang, *Anal. Bioanal. Chem.*, 2013, **405**, 8799.
24. Q. Liu, J. B. Shi, J. T. Sun, T. Wang, L. X. Zeng, G. B. Jiang, *Angew. Chem. Int. Ed.*, 2011, **50**, 5913.
25. J. W. Liu, Q. Zhang, X. W. Chen, J. H. Wang, *Chem. Eur. J.*, 2011, **17**, 4864.
26. R. Marcilla, J. A. Blazquez, J. Rodriguez, J. A. Pomposo, D. Mecerreyes, *J. Polym. Sci., Part A: Polym. Chem.*, 2004, **42**, 208.
27. J. W. Liu, Y. Zhang, X. W. Chen, J. H. Wang, *ACS Appl. Mater. Interfaces*, 2014, **13**, 10196.
28. Z. Lin, Z. W. Xia, J. N. Zheng, D. Zheng, L. Zhang, H. H. Yang, G. N. Chen, *J. Mater. Chem.*, 2012, **22**, 17914.
29. S. Carda-Broch, A. Berthod, D. W. Armstrong, *Anal. Bioanal. Chem.*, 2003, **375**, 191.
30. J. L. Chen, X. P. Yan, *J. Mater. Chem.*, 2010, **20**, 4328.
31. A. C. Ferrari, *Solid State Commun.*, 2007, **143**, 47.
32. A. C. Ferrari, J. C. Meyer, V. Scardaci, C. Casiraghi, M. Lazzeri, F. Mauri, S. Piscanec, D. Jiang, K. S. Novoselov, S. Roth, A. K. Geim, *Phys. Rev. Lett.*, 2006, **97**, 187401.
33. C. N. R. Rao, A. K. Sood, K. S. Subrahmanyam, A. Govindaraj, *Angew. Chem. Int. Ed.*, 2009, **48**, 7752.
34. R. Marcilla, J. A. Blazquez, R. Fernandez, H. Grande, J. A. Pomposo, D. Mecerreyes, *Macromol. Chem. Phys.*, 2005, **206**, 299.
35. Q. Liu, J. B. Shi, M. T. Cheng, G. L. Li, D. Cao, G. B. Jiang, *Chem. Commun.*, 2012, **48**, 1874.
36. Y. S. Al-Degs, M. I. El-Barghouthi, A. H. El-Sheikh, G. M. Walker, *Dyes Pigments*, 2008, **77**, 16.
37. F. X. Gao, X. L. Zhao, X. W. He, W. Y. Li, Y. K. Zhang, *Anal. Methods*, 2013, **5**, 6700.

38. A. Kosior, M. Antosova, R. Faber, L. Villain, M. Polakovic, J. *Membrane. Sci.*, 2013, **442**, 216.
39. K. Ralla, U. Sohling, D. Riechers, C. Kasper, F. Ruf, T. Scheper, *Bioproc. Biosyst. Eng.*, 2010, **33**, 847.
40. M. D. Stoller, S. J. Park, Y. W. Zhu, J. H. An, R. S. Ruoff, *Nano Lett.*, 2008, **8**, 3498.
41. Y. Shu, X. W. Chen, J. H. Wang, *Talanta*, 2010, **81**, 637.